Journal of Biomechanics 50 (2017) 130–137

Contents lists available at ScienceDirect

Journal of Biomechanics

journal homepage: www.elsevier.com/locate/jbiomech
www.JBiomech.com

Pressure drop and arterial compliance – Two arterial parameters in one measurement

Oren M. Rotman [a,b,*], Uri Zaretsky [a], Avraham Shitzer [c], Shmuel Einav [a,b]

[a] Department of Biomedical Engineering, Tel Aviv University, Tel Aviv 69978, Israel
[b] Department of Biomedical Engineering, Stony Brook University, Stony Brook, NY 11794, USA
[c] Faculty of Mechanical Engineering, Technion Israel Institute of Technology, Haifa 32000, Israel

ARTICLE INFO

Article history:
Accepted 2 November 2016

Keywords:
Arterial distensibility
Coronary
Atherosclerosis
Fractional flow reserve
Vulnerable plaque

ABSTRACT

Coronary artery pressure-drop and distensibility (compliance) are two major, seemingly unrelated, parameters in the cardiovascular clinical setting, which are indicative of coronary arteries patency and atherosclerosis severity. While pressure drop is related to flow, and therefore serves as a functional indicator of a stenosis severity, the arterial distensibility is indicative of the arterial stiffness, and hence the arterial wall composition. In the present study, we hypothesized that local pressure drops are dependent on the arterial distensibility, and hence can provide information on both indices. The clinical significance is that a single measurement of pressure drop could potentially provide both functional and bio-mechanical metrics of lesions, and thus assist in real-time decision making prior to stenting. The goal of the current study was to set the basis for understanding this relationship, and define the accuracy and sensitivity required from the pressure measurement system. The investigation was performed using numerical fluid–structure interaction (FSI) simulations, validated experimentally using our high accuracy differential pressure measurement system. Simplified silicone mock coronary arteries with zero to intermediate size stenoses were used, and various combinations of arterial distensibility, diameter, and flow rate were simulated. Results of hyperemic flow cases were also compared to fractional flow reserve (FFR). The results indicate the potential clinical superiority of a high accuracy pressure drop-based parameter over FFR, by: (i) being more lesion-specific, (ii) the possibility to circumvent the FFR dependency on pharmacologically-induced hyperemia, and, (iii) by providing both functional and biomechanical lesion-specific information.

1. Introduction

Arterial flow and compliance are used in the cardiovascular clinical setting, as indicators of coronary arteries patency and atherosclerosis severity.

Fractional flow reserve (FFR) has recently been established as the gold standard functional indicator for epicardial coronary lesions, utilizing trans-stenotic pressure measurement as a surrogate for flow under maximal hyperemia. This essentially estimates the ischemic severity of a lesion, regardless of its geometrical features, and is mostly useful for intermediate size stenoses (defined by cross-sectional areas of 40–70%), where coronary angiography sensitivity is limited (Tobis et al., 2007). The common clinical practice today is to stent lesions that reduce hyperemic flow and to avoid stenting those that do not reduce hyperemic flow (Pijls and Sels, 2012).

Arterial compliance (or distensibility) has been a primary measure for assessing arterial stiffness as an indicator for the arterial stenosis severity (Ovadia-Blechman et al., 2003), and distinguishing between white or yellow plaques (Takano et al., 2001). Atherosclerosis was correlated with impaired distensibility in comparison to normal healthy arteries (Mokhtari-Dizaji et al., 2006; van Popele et al., 2001), even in sites accompanying occult atherosclerosis, which could not be detected by conventional angiography (Nakatani et al., 1995).

Over the years, arterial pressure drop and distensibility were studied separately, as two independent parameters. Konala et al. have investigated the effect of coronary plaque compliance on pressure drop (Konala et al., 2011b) and FFR (Konala et al., 2011a)

Abbreviations: B.C., boundary conditions; CFR, coronary flow reserve; CMP, common mode pressure; FFR, fractional flow reserve; FSI, fluid–structure interaction; ρ, density [kg/m^3]; μ, fluid dynamic viscosity [Pa s]; ϑ, Poisson ratio; B, solid bulk modulus of elasticity [Pa]; K, fluid bulk modulus of elasticity [Pa]; σ, engineering stress [Pa]; λ, stretch; Re, Reynolds number; $P_d(t)$, time-dependent pressure drop [mmHg]; P_d-max, maximum component of $P_d(t)$ for a single cycle [mmHg]; P_d-$mean$, average component of $P_d(t)$ for a single cycle [mmHg]; $P_g(t)$, time-dependent Gauge pressure (blood pressure) [mmHg]

* Corresponding author at: Department of Biomedical Engineering, Stony Brook University, Stony Brook, NY 11794, USA.
E-mail address: orenrotman1@gmail.com (O.M. Rotman).

http://dx.doi.org/10.1016/j.jbiomech.2016.11.026
0021-9290/

for cases of severe stenoses (70–90%) during hyperemic flow using computational fluid–structure interaction (FSI) simulations. These studies, however, presented no information on FFR-relevant pressure drops for intermediate size stenosis. The present study hypothesizes that arterial pressure drop is dependent on the arterial distensibility, and seeks to investigate it through a combination of coronary flow rates and diameters, for zero to intermediate size stenoses. The motivation was the development of the capability to obtain both functional and biomechanical information from a single pressure measurement during cardiac catheterization that will assist in improving the decision making prior to stenting. While this manuscript refers mostly to coronary flow, it is also applicable to the entire arterial system.

2. Materials and methods

2.1. Computational model

2.1.1. Coronary models

Simplified coronary arteries were simulated as straight compliant tubes to match our experimental silicone models (Fig. 1). A 0.835 mm radius tube (r_c) was set concentrically along the lumen to depict a 5 French fluid-filled double-lumen catheter that was used in the experimental setup. The models were scaled up from a 3 mm coronary artery to a baseline diameter (D_0) of 5 mm to keep the simulations identical to the experimental model, utilize flow and pressure recordings as boundary conditions (B.C.), and subsequently validate the computational results. Scaling up the models in the experimental setup was necessary to allow sufficient measurements with the 5 French catheter within the stenosis models. The numerical models were divided into four sections along the planes of symmetry to save computational time. Fixed extensions were added on both sides of the compliant model to retain similarity to the experimental setup (40 cm rigid extension was added at the compliant tube inlet where flow was measured, to allow flow development at the inlet, and 5 cm rigid extension at the outlet where pressure was measured).

2.1.2. Governing equations and FSI formulation

The fluid flow interactions with the compliant tube were modeled using coupled continuity (Eq. (1)) and momentum (Eq. (2)) equations for incompressible, viscous, and laminar flow (Reynolds numbers are detailed in Section 2.1.6) along with the compliant tube wall stress equilibrium equation (Eq. (3)). The fluid was assumed slightly compressible (Eq. (4)) to allow for easier convergence of the models. The arbitrary Lagrangian–Eulerian formulation was used to solve Eqs. (1)–(3) subjected to the B.C. described in Section 2.1.3.

$$\nabla \cdot u = 0 \tag{1}$$

$$\rho\left(\frac{\partial u}{\partial t}+(u\cdot\nabla)u\right) = -\nabla P+\mu\nabla^2 u \tag{2}$$

$$\sigma^S_{ij,j} = 0 \tag{3}$$

$$\rho = \rho_0\left(1+\frac{P}{K}\right) \tag{4}$$

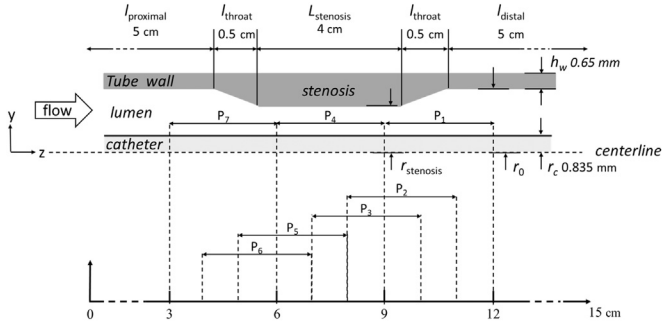

Fig. 1. Sketch of the mock coronary models' geometry. r_c is the catheter radius, h_w accounts for the wall thickness, $r_{stenosis}$ is the radius of the stenosis, and r_0 is the nominal radius of the tube. For zero stenosis cases $r_{stenosis}$ equals r_0.

where u is the fluid velocity [m/s], P is the pressure [Pa], μ is the dynamic viscosity of the fluid [Pa s], ρ is the fluid density [kg/m^3], ρ_0 is the density at $P = 0$ Pa, K is the fluid bulk modulus of elasticity [Pa], and σ^S_{ij} is the stress tensor for the compliant tube wall [Pa]. For the stenois models, the k-epsilon turbulence model was adopted since it provided the best matching between the computational and experimental pressure drops.

2.1.3. Boundary conditions

Three consecutive flow/pressure cycles, that were recorded from two matching experiments (normal or hyperemic flow), were set as B.C. Average velocity ($u(t)$) was set at the inlet, and pressure ($P_g(t)$) was set at the outlet, at the same locations where they were measured experimentally (Fig. 2). A relatively slow pulsation rate of 0.8 Hz (50 bpm) was used to allow enhanced stability of the pressure measurements in the experimental setup. It was critical to use recorded data as B.C. since the mechanical properties of the compliant model affect the pressure-flow phase-lag and hence the calculated pressure drops. The baseline pressure in the simulations ($P_g(t)$) was offset to zero to keep the nominal diameter of the tube (D_0) uniform throughout the simulations of each of the five diameters simulated (for varying ΔD cases). A no-slip condition was applied at the catheter wall–fluid interface, and at the compliant tube wall–fluid interface. In addition, the following B.C. were assumed:

$$\sigma^S_{ij}n_j = \sigma^F_{ij}n_j \quad \text{at the lumen – wall interface} \tag{5}$$

$$d^S = d^F \quad \text{at the inner wall} \tag{6}$$

$$\sigma^S_{ij}n_j = 0 \quad \text{stress – free state assumed at the outer wall} \tag{7}$$

$$d^S n_j = 0 \quad \text{on the wall symmetry planes} \tag{8}$$

$$d^S = 0 \quad \text{at the rigid wall extensions} \tag{9}$$

$$\frac{\partial u}{\partial n_j} = 0 \quad \text{on the lumen symmetry planes} \tag{10}$$

where d^S and d^F are the displacements of the solid and fluid domains [m], respectively, and σ^F_{ij} is the stress tensor for the fluid flow [Pa].

2.1.4. Material properties

The working fluid was distilled water–glycerol solution (volumetric ratio of 1:0.56 at room temperature) defined as Newtonian and slightly compressible (Mach number was 0.002 « 0.1). The dynamic viscosity was taken as $\mu = 3.8$ mPa s, as measured using a glass capillary viscometer (Canon-Fenske, No. T625, size 50, Canon® Instrument Company Inc., PA, USA). The fluid density was estimated as $\rho = 1100$ kg/m^3, and the bulk modulus $K = 10^9$ Pa (Cheng, 2008).

The silicone tube wall (MED-6020, Nusil Silicone Technology, CA, USA) was homogeneous, incompressible, and hyperelastic using the first order Mooney–Rivlin model (HE model in Rotman et al. (2015)):

$$\sigma = 2\left(C_1+\frac{C_2}{\lambda}\right)\left(\lambda-\frac{1}{\lambda^2}\right) \tag{11}$$

where σ is the engineering stress [Pa], λ is the stretch, and $C_1 = 33{,}300$ Pa and $C_2 = 27{,}100$ Pa are the material constants. The material properties were $\rho = 1050$ kg/m^3, bulk modulus of $B = 1.5$ GPa, and Poisson ratio of $\vartheta = 0.49$. Varying distensibility (ΔD) cases were simulated by adjusting the slope of the silicone stress–strain curve. For the stenoses cases, only the material properties of the plaque region were adjusted (Table S1).

2.1.5. Meshing and numerical model

The models were meshed with 8-node brick elements in both the solid and fluid domains (Table S2). Large deformations and large strains were considered for the solid elements. The coupled FSI equations employing a direct scheme were solved by the finite element code ADINA (ADINA R&D Inc., Watertown, MA, USA). A time discretization of 10 ms was selected, since it yielded the best agreement between the calculated and the experimental pressure drops. Mesh convergence check was performed to ensure that the solutions of the pressure drop values in each case differed by no more than 0.005 mmHg.

2.1.6. Simulation plan

In investigating the local fluid pressure as affected by the tube distensibility, diameter and flow rate, it is important first to understand these relationships in a straight tube without stenosis. Therefore, in addition to the scaled-up baseline diameter of 5 mm, four additional diameters were simulated for the zero-stenosis cases (4.70, 4.85, 5.15, and 5.30 mm), taking into account matching dimensional analysis; peak Reynolds (Re) of ~200 and ~800 (Konala et al., 2011b) for normal